RESEARCH ARTICLE | FEBRUARY 05 2019

Fusion-bonding behavior of plasticized corn proteins in fused deposition modeling process

Laurent Chaunier; Benoît Duchemin; Estelle Couallier; Guy Della Valle; Denis Lourdin; Anne-Laure Reguerre; Eric Leroy

AIP Conf. Proc. 2065, 030055 (2019)
https://doi.org/10.1063/1.5088313

Fusion-Bonding Behavior of Plasticized Corn Proteins in Fused Deposition Modeling Process

Laurent Chaunier[1,2,a)], Benoît Duchemin[3,b)], Estelle Couallier[2,c)], Guy Della Valle[1,d)], Denis Lourdin[1,e)], Anne-Laure Reguerre[1,f)] and Eric Leroy[2,g)]

[1]*INRA, BIA, UR 1268, La Géraudière. 44316 Nantes Cedex 3, France*
[2]*CNRS, UBL, GEPEA, UMR 6144, CRTT, 37 av. de l'université. 44602 St-Nazaire Cedex, France*
[3]*Normandie Université, ULH, CNRS, LOMC, UMR 6294, 76600 Le Havre, France*

[a)]*Corresponding author: laurent.chaunier@inra.fr*
[b)]*benoit.duchemin@univ-lehavre.fr*
[c)]*estelle.couallier@ univ-nantes.fr*
[d)]*Guy.Della-valle@inra.fr*
[e)]*Denis.Lourdin@inra.fr*
[f)]*anne-laure.reguerre@inra.fr*
[g)]*Eric.Leroy@univ-nantes.fr*

Abstract. The processing of natural biopolymers by Fused Deposition Modeling (FDM) opens perspectives for applications in food and health domains by taking advantages of their edibility, biocompatibility and bioresorbability. Glycerol plasticized zeins (proteins from maize kernels) present thermomechanical properties matching the extrusion step requirements of FDM (at $T_{printing}$=130°C for 20% of glycerol). The present work focuses on the fusion-bonding step of the process between adjacent filaments. Mechanisms at the root of the thermal bonding of amorphous polymers at $T>T_g$ are governed by melt's surface tension (Γ, driving force) and viscosity (η, limiting force). In addition, healing phenomenon, assessed by the degree of healing, Dh, increases with time as $Dh \propto t^{1/4}$. It originates from the diffusion of polymer chains across the interface in accordance with the reptation theory. Dynamic rheological properties of molten extruded filaments of plasticized zeins were determined in a pre-heated oscillatory rheometer at 130°C, with $|\eta^*|_{\dot{\gamma}=1.6s^{-1}}$ ranging from 0.6 to 0.8kPa.s. Γ was estimated from the evolution of the fusion-bonding neck growth between two extrudates (polymer sintering model). The 0.1mm.s^{-1} bonding rate observed at 130°C allowed estimating a melt surface tension of 30-40mN.m^{-1}. Concurrently surface energy measurements were conducted on solid plasticized zein at 20°C using the sessile drop method: By varying liquids deposited on zein-based surface and following Owens and Wendt's approach, γ_{SV} was found to amount to 39.2±1.6mN.m^{-1}, with the dispersive component γ_{SV}^d=4.2±0.4mN.m^{-1} and the polar one γ_{SV}^p=35.0±1.2mN.m^{-1}. These values were used to extrapolate a melt surface tension using the typical surface tension dependence $d\gamma/dT \approx -0.05$mN.m^{-1}.K^{-1} like for synthetic polymers following the Eötvös' law. The extrapolated values at 130°C were in agreement with those obtained from fusion-bonding experiments.

Keywords: Additive Manufacturing, Biopolymer, Rheology, Sintering, Surface tension, Zeins

PACS: 68, 81, 83

INTRODUCTION

Zein is a model-material for investigating the deposition of biopolymers in the molten state. Zein is a storage protein belonging to the prolamins group [1]. It amounts to about 5% of the dry weight of corn kernel. It is an abundant by-product of starch extraction that can be used as an edible water barrier in foods and for the production of degradable plastics. Zeins can be thermoplasticized by blending with non-volatile compounds as glycerol and submitted to thermomechanical treatments like extrusion [2, 3]. It was shown to present a shear-thinning behavior in the molten state, with possible stiffening during thermomechanical treatments due to thermal aggregation and crosslinking with a gel-point. For short residence times in the molten state, rheological properties of are similar to those of standard polymers used for Fused Deposition Modeling (FDM), opening perspectives to target the 3D deposition of this biopolymer in the molten state [4, 5].

Proceedings of PPS-34
AIP Conf. Proc. 2065, 030055-1–030055-5; https://doi.org/10.1063/1.5088313
Published by AIP Publishing. 978-0-7354-1793-9/$30.00

The present work is dedicated to the evaluation of properties governing the fusion-bonding behavior of plasticized zein extruded FDM filaments. A model of the thermal sintering sequence mimicking their adhesion once deposited is used, allowing evaluating the surface tension of the melt.

Four main steps are involved during amorphous polymer sintering (Fig.1): Due to molecular mobility, the initial contact line between adjacent filaments leads to the creation of a bonding neck which grows by the interdiffusion of polymer chains across the interface, until randomization of polymeric chains, for long healing time at high temperature [6, 7].

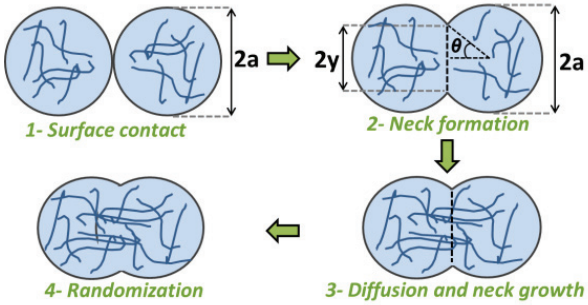

FIGURE 1. Schematic representation of fusion-bonding steps for a thermoplastic amorphous polymer at $T>T_g$

For a temperature $T>T_g$, the neck growth rate impacting the final degree of bonding can be modelled by a modified Frenkel's model [8, 9]. It is based on the evolution of the bonding angle, θ, measured between the equator of adjacent extruded filaments and the limit of their bonding front (Fig. 1):

$$\frac{d\theta}{dt} = \frac{\Gamma}{a_0.\eta}.\frac{2^{-\frac{5}{3}}.\cos(\theta).\sin(\theta).(2-\cos(\theta))^{\frac{1}{3}}}{(1-\cos(\theta)).(1+\cos(\theta))^{\frac{1}{3}}} \quad \text{with} \quad \theta = \sin^{-1}(\frac{y}{a}) \qquad (1\&2)$$

In this model that was successfully applied to synthetic polymers sintering [7, 8, 13], two key properties of the melt are involved: viscosity and surface tension. The melt viscosity limits the coalescence of the polymers. The complex viscosity moduli $|\eta^*|$ were reported to amount from about 0.6 to 1.2kPa.s at low shear rate ($\dot{\gamma}$=1.6s^{-1}, or 10rad.s^{-1}) in the case of standard polymers for FDM: PLA and ABS at their processing temperatures (190°C and 240°C, respectively). Their surface tension, Γ, is a driving force during the sintering sequence, with typical values reported from about 20 to 40mN.m^{-1} for synthetic polymers melts [9-13]. We will use the same approach to model the fusion-bonding behavior of plasticized zein and to evaluate its melt surface tension which will be compared to extrapolated values from surface energy measurements on solid zein.

MATERIALS AND METHODS

Raw Materials, Thermomolding and Extrusion

Zein from maize (Ref.Z3625) and glycerol were purchased from Sigma-Aldrich (F-38, Saint-Quentin Fallavier). The moisture content was determined by thermogravimetry after 2h at 130°C (TA Instruments, F-78 Guyancourt). A zein-based plasticized composition was obtained after blending with 20% glycerol (w/w), namely "Z20Gly". It was thermomolded as flat cylindrical samples for the subsequent determination of contact angles with sessile drops ($Ø_{molded\_cylinder}$=16mm, $h_{molded\_cylinder}$≈3mm). It was also extruded as filaments at 130°C, to carry out fusion-bonding and thermomechanical trials on cylindrical extrudates ($Ø_{extrudate}$≈2mm).

Glass Transition and Thermomechanical Properties of Zein-based materials

To determine the glass transition temperature, thermograms were recorded with an automated Differential Scanning Calorimeter DSC (Q100, TA Instruments, F-78 Guyancourt). Each specimen (10 mg) was placed into a sealed stainless-steel cell. Measurements were performed at 3°C/min from 10 to 140°C during a second scan, to cancel thermal events due to aging during storage. Extruded filaments cut in 20mm long specimen were submitted to Dynamic Mechanical Analysis in tensile mode (DMA-50N-O1dB Model, Metravib, F-59 Lyon). The mechanical active length between the grips was 10mm and extrudates were characterized at 1Hz by DMA, with a strain set at 0.1% and heating rate of 3°C/min, up to 180°C.

Rheology, Surface Tension and Sintering Sequence

The rheological properties of extruded plasticized zein (Z20Gly) have been determined with a controlled strain rotational rheometer MARSIII (Thermo Scientific GmbH, Karlsruhe-DE) between parallel plates (Ø=20mm, gap≈1.5mm). It was preliminary pre-heated at 130°C by Peltier effect cell allowing the immediate heating of the specimen. The normal force applied during the measurement was F_N=0.5N, the solicitation frequency ν=1.6Hz (ω=10 rad.s^{-1}) and the strain was γ_0=0.7% (checked to be in the linear domain).

Contact angle measurements were carried out with sessile drops from 3 liquids: water, ethanol and ethylene glycol (Fig. 2-a; Table 1). Drops were placed on the surface of thermomolded flat samples presenting neat surfaces and the contact angles were measured from images acquired using a DSA-30 tensiometer (Drop Shape Analysis; Krüss GmbH, Hamburg, DE). This was repeated 12 times in the same conditions for each liquid. The surface tension of the solid substrate and the critical surface tension of liquid to spread on it were determined as following Owens and Wendt's approach based on Young's law (Eq. 3 and 4), followed by Zisman plot technique [14]:

$$\gamma_{SV}=\gamma_{SL}+\gamma_{LV}.\cos(\theta_e) \quad \text{and} \quad (1+\cos(\theta_e)).\gamma_{LV} = 2.[\sqrt{\gamma_{LV}^d.\gamma_{SV}^d}+\sqrt{\gamma_{LV}^p.\gamma_{SV}^p}] \qquad (3\&4)$$

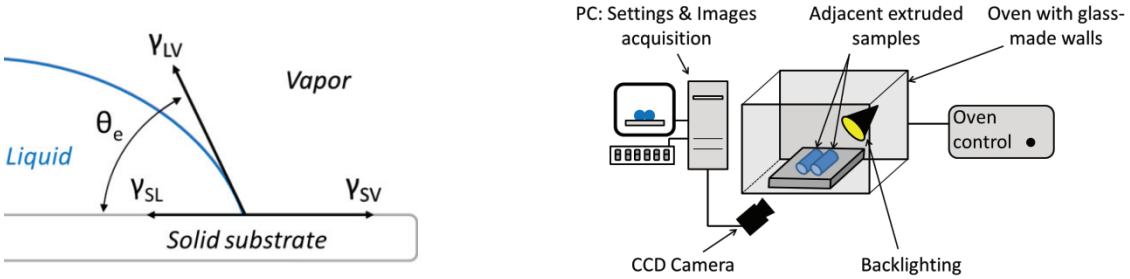

(a) (b)

FIGURE 2. Schematic representation of the contact angle determined at the equilibrium, θ_e [°], after deposition of a liquid drop on a solid surface: γ_{LV}, liquid surface tension; γ_{SV}, solid surface tension; γ_{SL}, interfacial tension between solid and liquid; with $\gamma_{SV}=\gamma_{SL}+\gamma_{LV}.\cos(\theta_e)$ (a). Scheme of the experimental device to acquire images during fusion-bonding sequence (b)

A transparent oven was used to monitor sintering sequences between two zein-based extrudates at constant temperature (Fig. 2-b). Images obtained with a CCD camera were segmented with an automatic thresholding in gray level, followed by the determination of the length of the bonding neck (vertical of minimum length between the two cylinders). The image treatment routine was programmed in Matlab®. Then, the surface tension of the molten material (Γ_{melt}) was computed by applying the sintering model (Eq. 1 & 2).

TABLE (1). Surface tension and density of the different liquids used to depose sessile drops

Liquid	Surface tension γ_{LV} [mN.m^{-1}]	Disperse part γ_{LV}^d [mN.m^{-1}]	Polar part γ_{LV}^p [mN.m^{-1}]	Density [-]
Water	72.8	26.0	46.8	0.998
Ethylene glycol	47.7	26.4	21.3	1.109
Ethanol	22.1	17.5	4.6	0.789

RESULTS AND DISCUSSIONS

Once equilibrated at standard humidity level (RH=59%, leading to a water content of ~7 wt. %), extruded filaments based on Z20Gly are in the vitreous state, with an elastic modulus E' measured at about 1GPa at 20°C. When heated, extrudates present a main mechanical relaxation, linked to their glass transition at T_g=42°C as assessed by DSC. The value of E′ drops to about 0.6 MPa at 130°C, with a possible flowing at this temperature. It is also a convenient compromise to obtain fluid melts from plasticized zein, without altering the material and avoiding bubbles due to vaporisation of water potentially later acting as defects in the consolidated material.

When reaching immediately the molten state at 130°C, extrudates present a viscoelastic behavior with a low viscosity |η*| ranging from 0.6 to 0.8kPa.s after 20 to30s at 130°C (Fig. 3-a).

For longer time, it increases above 1kPa.s after 100s, because of proteins thermal aggregation. Thanks to the images acquired during the sintering sequence at 130°C, the growth rate of the bonding neck could be quantified (Fig. 3-b and -c) with values ranging from 0.1 to 0.13mm.s^{-1}. Applying the sintering model (Eq. 1 & 2), with the above viscosity values, this leads to a melt surface tension, Γ_{melt}, ranging from 30 to 40mN.m^{-1}.

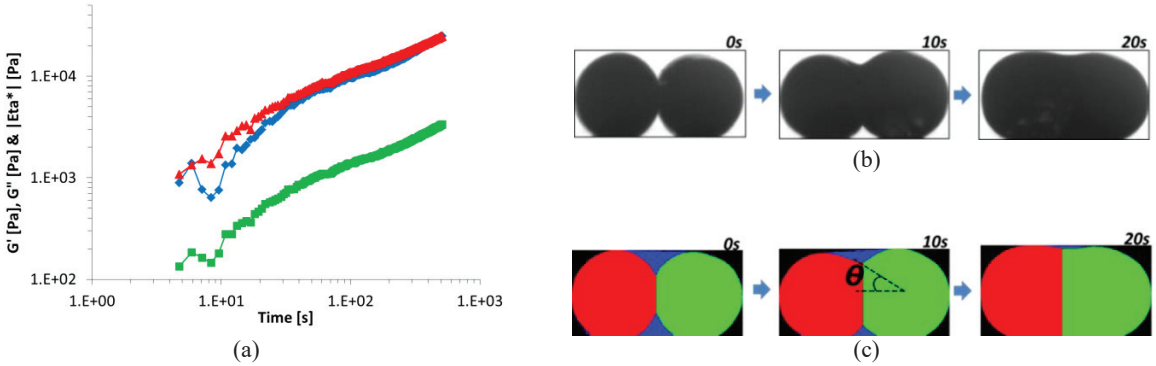

(a) (b) (c)

FIGURE 3. Rheological properties of molten extruded plasticized zein (Z20Gly) in a pre-heated oscillatory rheometer at T=130°C (G′ (♦), G″(▲) and |η*|(■)) (a). Images acquired during a fusion-bonding sequence at 130°C for extruded filaments based on zein -Z20Gly- ($Ø_{extruded\_cylinder}$≈2mm, $L_{extruded\_cylinder}$≈5mm) (b). Images treatment after segmentation: determination of zones coming from each of the two initial extruded cylinders (in red and green from the initial image), separated by the vertical minimum length (being the fusion-bonding neck). Example of determination of the bonding angle θ, for t=10s (for fueling the sintering model presented in Eq.1&2) (c)

Concurrently, the sessile drop experiments conducted on solid glycerol plasticized zein show an evolution of the contact angle with the surface tension of liquids close to that of measurements carried out on zein-based resins plasticized with sugars [13]. Indeed, the critical surface tension of a deposited liquid can be extrapolated at γ_{LVc} =13.3mN.m^{-1}, below which its total spreading could be obtained on the solid surface (Fig. 4). It is also close to the value found for zein plasticized with glucose and galactose in a previous work (γ_{LVc}=11 and 13mN.m^{-1}, respectively; [13]). Furthermore, the surface tension of Z20Gly in the solid state is found at γ_{SV}=39.2±1.6mN.m^{-1} at room temperature following Owens and Wendt's approach (with a disperse part at γ_{SV}^{d}=4.2±0.4mN.m^{-1} and a polar part at γ_{SV}^{p} =35.0±1.2mN.m^{-1}).

This surface tension is comparable to that of standard polymers for FDM under similar conditions: γ_{SV}=43mN.m^{-1} for PLA [15] and about 42mN.m^{-1} for ABS [16, 17]. Results obtained for surface tension of zein-based materials in the solid state are close to those of synthetic polymers used in the biomedical domain. That may explain the application of zein-based materials in the biomedical and pharmaceutical domains, where materials surface properties are determinant, especially concerning cell adhesion and biocompatibility [17, 18].

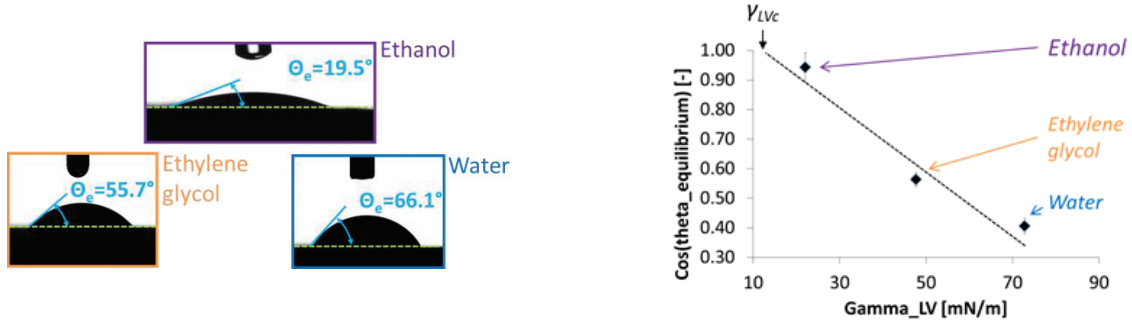

(a) (b)

FIGURE 4. Images of sessile drops and determination of the equilibrium angle in the case of three liquids deposited on the solid zein-based material (Z20Gly thermomolded as cylinder $Ø_{molded\_cylinder}$=16mm, $h_{molded\_cylinder}$≈3mm) at room temperature (a). Zisman plot, cos(θ_e)=f(γ_{LV}), for the determination of the liquid critical surface tension, γ_{LVc} (b)

In the molten state, the surface tension of polymers is rather low. It ranges from about 20 to 40mN.m^{-1}, and it was depicted to decrease quasi-linearly with temperature as described using the Eötvös' law. Indeed, for synthetic polymers, like polyethylene (PE), polystyrene (PS) or polypropylene (PP), values were obtained at about $d\gamma/dT$=-0.04 to -0.05mN.m^{-1}.K^{-1} [19]. Similar trends were reported for both amorphous (*e.g.* PS) and semi-crystalline polymers (*e.g.* PE) [20, 21]. In the case of standard polymers for FDM, γ decreases for PLA from about 40mN.m^{-1} at 20°C to 28mN.m^{-1} at 180°C, its printing temperature [15, 22]. As following the same trend, the decrease rate can be estimated at $d\gamma/dT\approx$-0.06 mN.m^{-1}.K^{-1} for the amorphous ABS, with values from 42mN.m^{-1} at 20°C to 29mN.m^{-1} at 240°C, its processing temperature [8, 9, 16]. By applying same rate to the surface tension of the plasticized zein-based material, from values determined by sessile drop method at ambient conditions, we obtain values ranging from 34 to 35mN.m^{-1} at 130°C. Such results are in the same range as those previously determined using the sintering model and the images acquired during the fusion-bonding sequence.

CONCLUSIONS AND MAIN PROSPECTS

The sintering model used for the characterization of the fusion-bonding behavior of FDM polymers was successfully applied to plasticized corn proteins, allowing the evaluation of the melt surface tension of this biopolymer. The values obtained are comparable with those of synthetic polymers at their processing temperature, and in the same range of magnitude as values extrapolated from solid state measurement using the Eötvös' law. These results have now to be completed by the evaluation of the thermal properties of zein-based materials, to reach a better understanding and modelling of their deposition in the molten state. This is especially of importance to target cohesive 3D parts based on this biopolymer dedicated to the controlled release of active ingredients, where the final porosity has to be sharply governed by process.

ACKNOWLEDGMENTS

The authors would like to thank Roselyne Désirest (INRA, Nantes) and Yannick Madec (UBL, IUT Carquefou) for their helpful contributions to samples extrusion and characterization.

REFERENCES

1. T.J. Anderson and B.P. Lamsal, *Cereal Chemistry* **88**(2), 159-173 (2011).
2. E. Corradini, E. S. de Medeiros, A. J. F. Carvalho, A. A. S. Curvelo and L. H. C. Mattoso, *Journal of Applied Polymer Science* **101**(6), 4133-4139 (2006).
3. G. W. Selling and K. D. Utt, *Polymer Degradation and Stability* **98**(1), 184-189 (2013).
4. L. Chaunier, G. Della Valle, M. Dalgalarrondo, D. Marion, D. Lourdin and E. Leroy, *Rheologica Acta* **56**(11), 941-953 (2017).
5. L. Chaunier, S. Guessasma, S. Belhabib, G. Della Valle, D. Lourdin and E. Leroy, *Additive Manufacturing,* **21**, 220-233 (2018).
6. C. A. Butler, R. L. McCullough and J. W. Gillespie. *Journal of Thermoplastic Composite Materials,* **11**(4)*,* 338-363 (1998).
7. C. Bellehumeur, M. Kontopoulou and J. Vlachopoulos. *Rheologica Acta* **37**(3), 270-278 (1998).
8. C. Bellehumeur, L. Li, Q. Sun and P. Gu. *Journal of Manufacturing Processes* **6**, 170-178 (2004).
9. Q. Sun, G. Rizvi, C. Bellehumeur and P. Gu. *Rapid Prototyping Journal* **14**(2), 72-80 (2008).
10. G. P. Kar, S. Biswas and S. Bose, *Physical Chemistry Chemical Physics* **17**, 1811-1821 (2014).
11. S. W. Hwang, D. H. Park, D. H. Kang, S. B. Lee and J. K. Shim, *Journal of Applied Polymer Science,* **133**(18), 10-15 (2016).
12. J. Vera, E. Contraires, M. Larochette, A. C. Brulez, S. Valette, and S. Benayoun, *Applied Surface Science,* **410**, 87-98 (2017).
13. S. Bakrani, F. Chabert, V. Nassiet, A. Cantarel and C. Garnier, *Proceedings of the International Conference ESAFORM* (2017).
14. B. Ghanbarzadeh, M. Musavi, A. R. Oromiehie, K. Rezayi, K., E. R. Rad and J. Milani, *Lwt-Food Science and Technology,* **40**(7), 1191-1197 (2007).
15. G. Biresaw and C.J. Carriere*, Journal of Polymer Science Part B-Polymer Physics,* **40**(19), 2248-2258 (2002).
16. J. Du, Z. Y. Wei, X. Wang, J. J. Wang and Z. Chen, *Journal of Materials Processing Technology,* **234**, 332-341 (2016).
17. F. Awaja, M. Gilbert, G. Kelly, B. Fox and P. J. Pigram (2009). *Progress in Polymer Science*, **34**(9), 948-968 (2009).
18. E. Corradini, P. S. Curti, A. B. Meniqueti, A. F. Martins, A. F. Rubira and E.C. Muniz. *International Journal of Molecular Sciences* **15(12)**, 22438-22470 (2014).
19. D. Y. Kwok, L. K. Cheung, C. B. Park and A.W. Neumann, *Polymer Engineering and Science,* **38**(5), 757-764 (1998).
20. S. Wu, *Journal of Physical Chemistry,* **74**(3), 632-640 (1970).
21. S. Wu, *Journal of Colloid and Interface Science,* **31**(2), 153-160 (1969).
22. E. J. Dil, M. Arjmand, Y. Li, U. Sundararaj and B. D. Favis, *European Polymer Journal,* **85**, 187-197 (2016).